

Supplementary Information: Distinction of lymphoid and myeloid clonal hematopoiesis

Abhishek Niroula^{1,2,3}, Aswin Sekar², Mark A. Murakami², Mark Trinder^{1,4}, Mridul Agrawal², Waihay J. Wong^{1,5}, Alexander G. Bick^{1,6}, Md Mesbah Uddin^{1,7}, Christopher J. Gibson^{1,2}, Gabriel K. Griffin^{1,5}, Michael C. Honigberg^{1,8}, Seyedeh M. Zekavat^{1,9}, Kaavya Paruchuri^{1,7,8,10}, Pradeep Natarajan^{1,7,10}, Benjamin L. Ebert^{*1,2,11}

Author affiliations

¹Broad Institute of MIT and Harvard, Cambridge, MA, USA

²Department of Medical Oncology, Dana-Farber Cancer Institute, Boston, MA, USA

³Department of Laboratory Medicine, Lund University, Lund, Sweden

⁴Center for Heart Lung Innovation, University of British Columbia, Vancouver

⁵Department of Pathology, Brigham and Women's Hospital, Boston, MA, USA

⁶Division of Genetic Medicine, Department of Medicine, Vanderbilt University Medical Center, Nashville, TN, USA

⁷Cardiovascular Research Center, Massachusetts General Hospital, Boston, MA, USA

⁸Cardiology Division, Massachusetts General Hospital, Boston, MA, USA

⁹Yale University School of Medicine, New Haven, CT, USA

¹⁰Department of Medicine, Harvard Medical School, Boston, MA, USA

¹¹Howard Hughes Medical Institute, Bethesda, MD, USA

*Correspondence:

Benjamin L. Ebert

Dana-Farber Cancer Institute

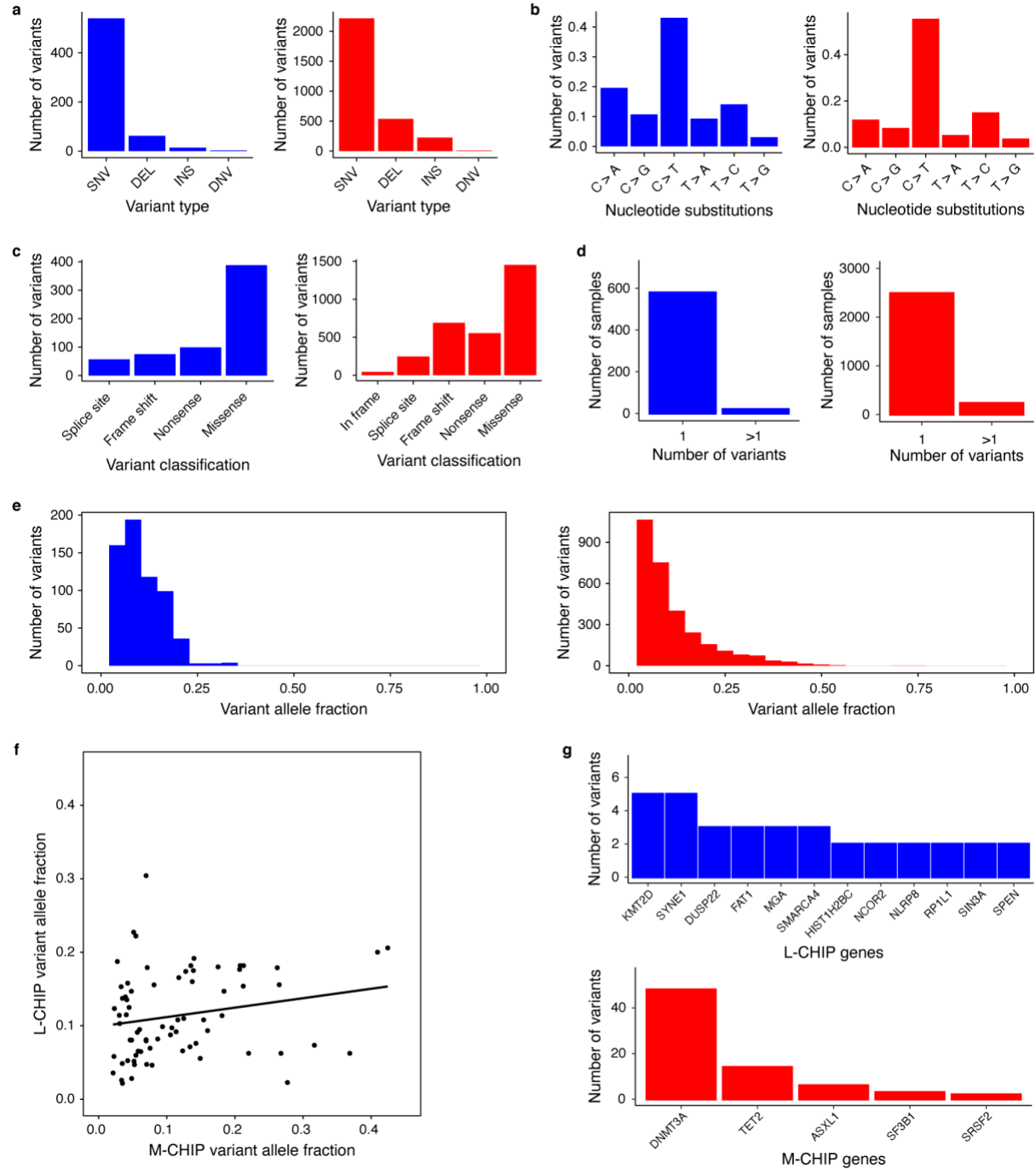
450 Brookline Ave, D1610A

Boston, MA 02215

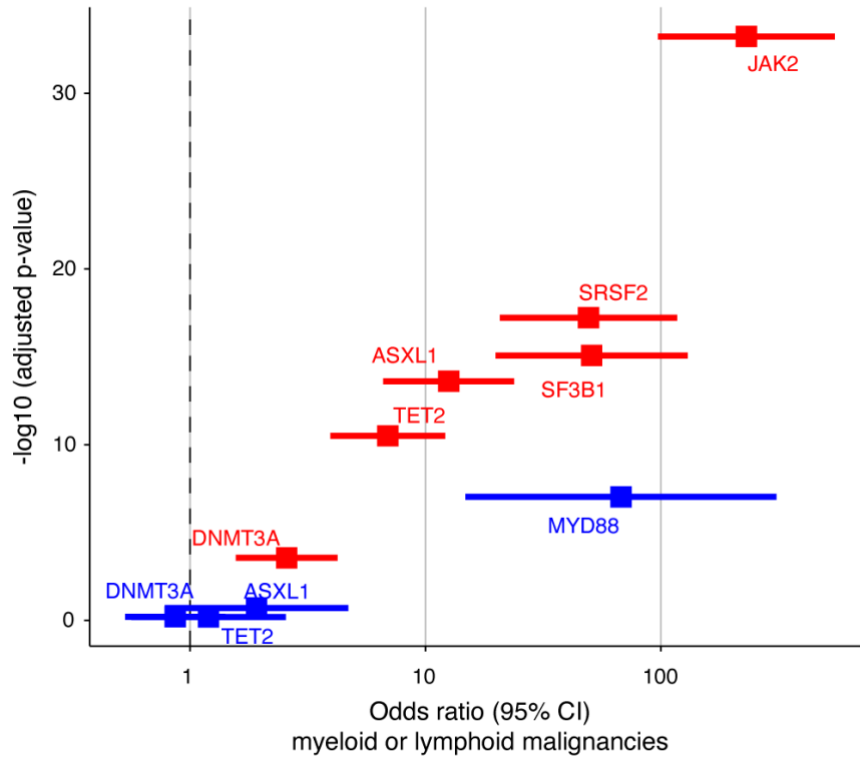
Tel: 617-632-1902

Email: benjamin_ebert@dfci.harvard.edu

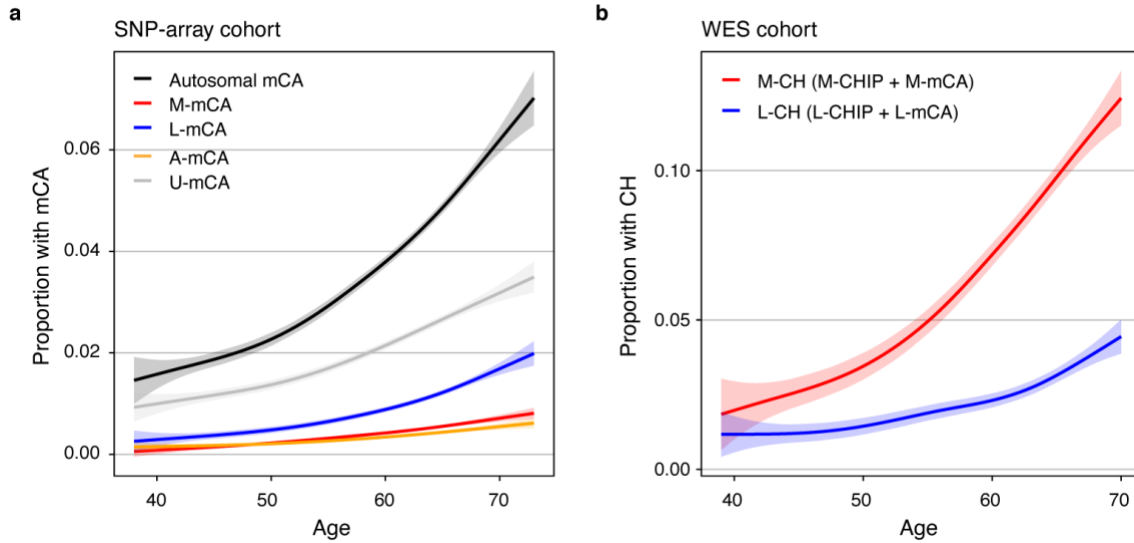
Supplementary Figures



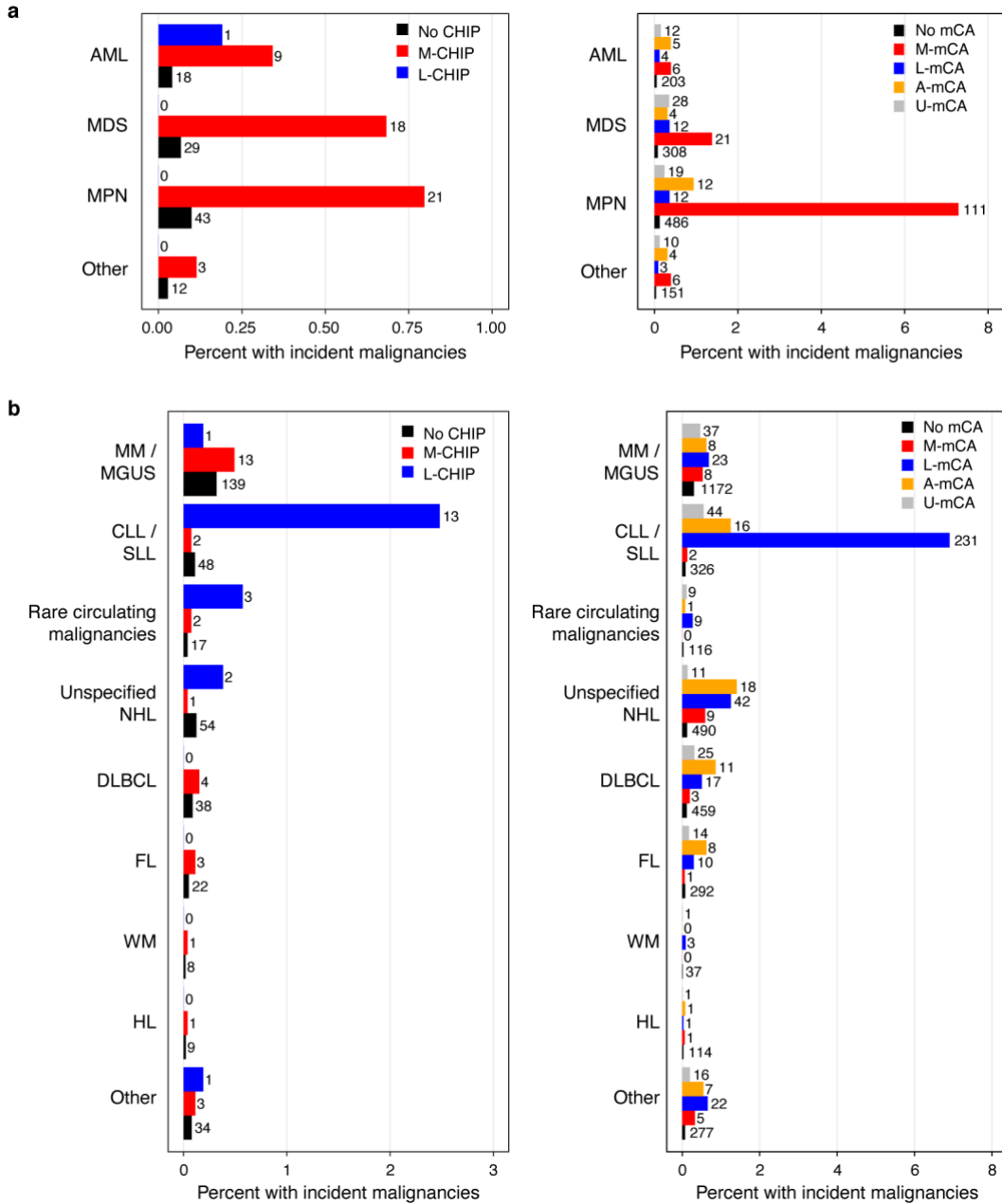
Supplementary Figure S1: Characteristics of somatic variants detected in myeloid and lymphoid driver genes. **a**) variant type, **b**) nucleotide substitutions for single nucleotide substitutions, **c**) variant classification based on changes in canonical protein sequence, **d**) number of variants detected per individual, **e**) variant allele fraction (VAF) of variants. Characteristics of M-CHIP are shown in red and L-CHIP in blue. **f**) Correlation between clone sizes of M-CHIP and L-CHIP detected in the same individual (n=73). **g**) Myeloid and lymphoid genes mutated among individuals carrying both M-CHIP and L-CHIP.



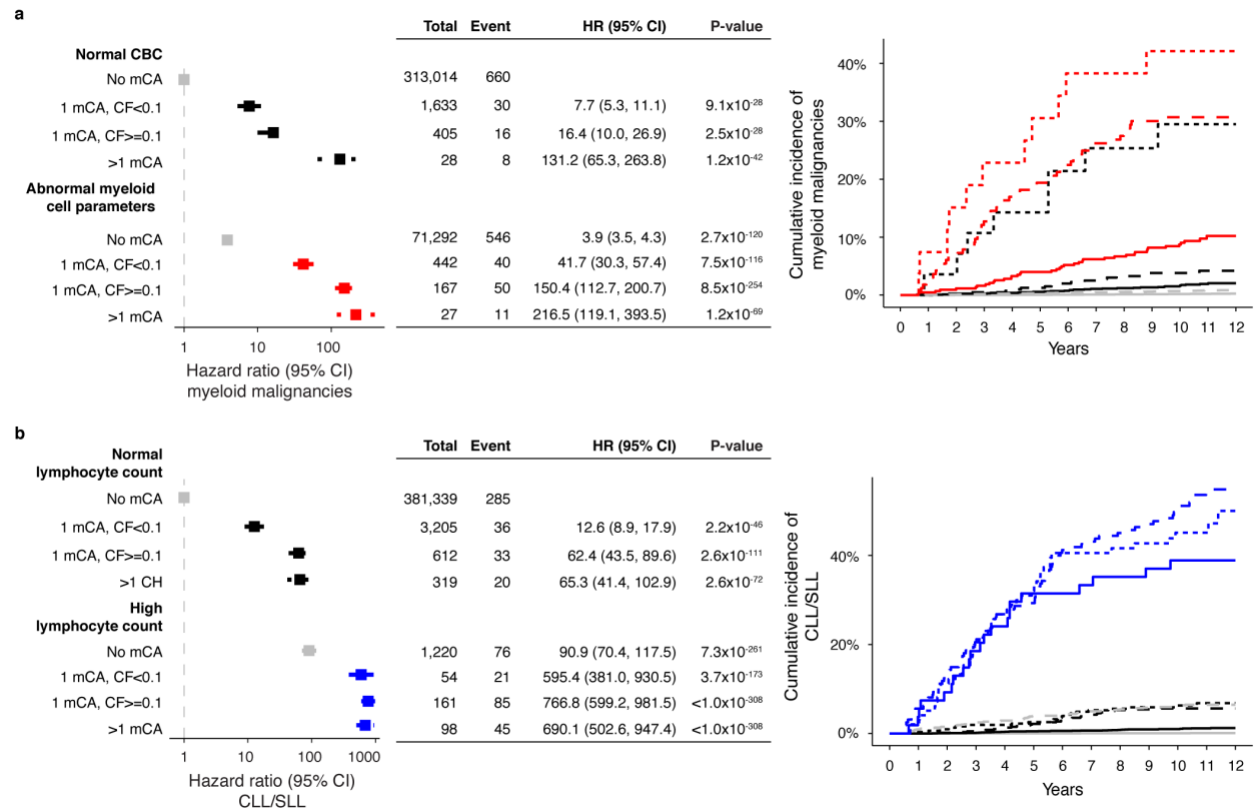
Supplementary Figure S2: Enrichment of CHIP gene mutations in myeloid and lymphoid malignancies. CHIP genes associated with myeloid (red) and lymphoid (blue) malignancies. Only genes mutated in at least 3 individuals who developed an incident myeloid or lymphoid malignancy between six months and 12 years after blood sample collection were analyzed. Tested genes were *DNMT3A* (n=1,827, n myeloid malignancies=18, and n lymphoid malignancies=17), *TET2* (n=510, n myeloid malignancies=14, and n lymphoid malignancies=7), *ASXL1* (n=201, n myeloid malignancies=11, and n lymphoid malignancies=5), *SRSF2* (n=34 and n myeloid malignancies=7), *SF3B1* (n=28 and n myeloid malignancies=6), *JAK2* (n=23, n myeloid malignancies=11), and *MYD88* (n=7, n lymphoid malignancies=3). Data are presented as odds ratio and 95% confidence intervals, computed by generalized linear regression model adjusting for age, age squared, sex, and smoking. CI, confidence interval.



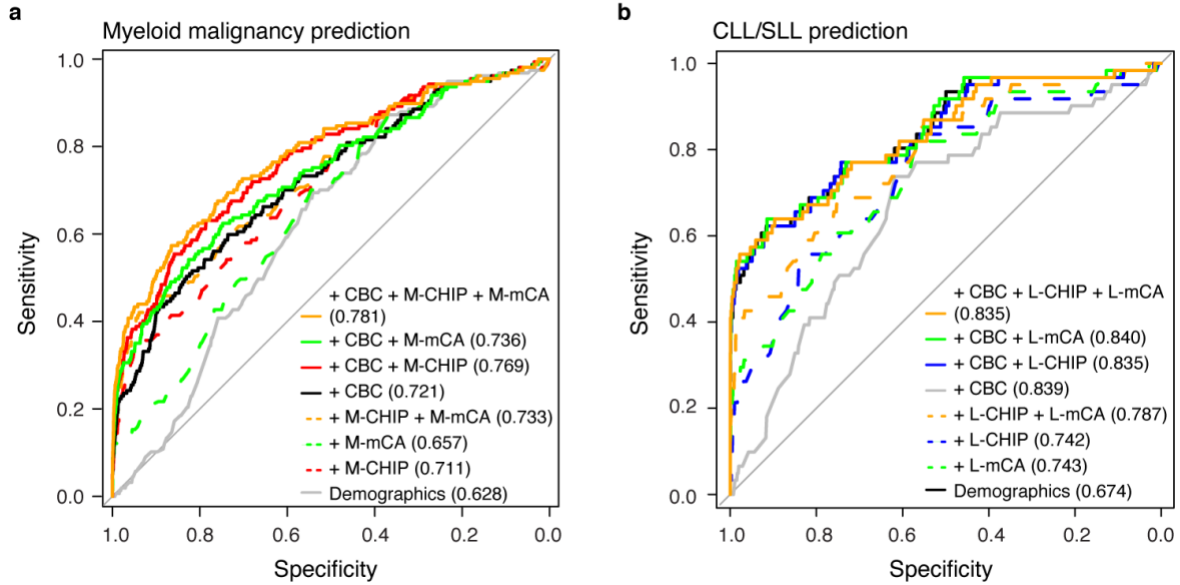
Supplementary Figure S3: Prevalence of CH increases with age. a) All four categories of mCAs are associated with age. The A-mCA (n=1278) is the rarest category of mCAs followed by M-mCA (n=1523), and L-mCA (3345). A large fraction of the mCAs remained unclassified (U-mCA, n=7966). **b)** Frequency of myeloid CH (M-CHIP + M-mCA, n=2975) and lymphoid CH (L-CHIP + L-mCA, n=1045) in the UKB WES cohort. **(a-b)** Data is fit with the general additive model using cubic regression splines and the shaded bands indicate the estimated 95% confidence interval.



Supplementary Figure S4: Enrichment of myeloid and lymphoid malignancy sub-types among individuals with CH. **a)** Frequencies of myeloid malignancy sub-types among CH cases and controls. **b)** Frequencies of lymphoid malignancy sub-types among CH cases and controls. The numbers above the bars indicate the total number of individuals with incident malignancy in those groups. The individuals are categorized based on the first coded hematologic malignancies. MDS, myelodysplastic syndrome; AML, acute myeloid leukemia; MPN, myeloproliferative neoplasms; CLL, chronic lymphocytic leukemia; SLL, small lymphocytic lymphoma; MM, multiple myeloma; MGUS, monoclonal gammopathy of undetermined significance; NHL, non-Hodgkin’s lymphoma; DLBCL, diffuse large B-cell lymphoma; FL, follicular lymphoma; WM, Waldenstrom’s macroglobulinaemia; HL, Hodgkin’s lymphoma; U-mCA, unclassified mCAs.



Supplementary Figure S5: Integration of mCA and blood cell indices stratify risk for developing hematologic malignancies. a) Myeloid CH (M-mCA/A-mCA) and abnormal myeloid cell parameters increase risk of myeloid malignancies. **b)** Lymphoid CH (L-mCA/A-mCA) and elevated lymphocyte count increase risk of CLL/SLL. **(a-b)** Since A-mCA were associated with risk of both myeloid and lymphoid malignancies, these are combined with M-mCA in the analysis of myeloid malignancies and with L-mCA in the analysis of lymphoid malignancies. Data are presented as hazard ratio and 95% confidence intervals, computed by using Cox proportional hazards model adjusting for age, sex, smoking, genetic ethnic ancestry, and genetic principal components 1-5. Red blood cell counts, platelet counts, and neutrophil counts were used to define individuals with abnormal myeloid cell parameters. CBC, complete blood count; HR, hazard ratio; CI, confidence interval; CLL, chronic lymphocytic leukemia; SLL, small lymphocytic lymphoma; VAF, variant allele fraction; CF, cell fraction.



Supplementary Figure S6: Integration of CH abnormalities and CBC predict the risk of myeloid malignancies and CLL/SLL. **a)** Sensitivity and specificity for predicting the incidence of myeloid malignancies computed by 10-fold cross-validation. Individuals with a diagnosis of myeloid malignancy (n=157) and those that did not have a diagnosis of myeloid or lymphoid malignancies (n=44781) were used for training and testing. **b)** Sensitivity and specificity for predicting the incidence of CLL/SLL computed by 10-fold cross-validation. Individuals with a diagnosis of CLL or SLL (n=61) and those that did not have a diagnosis of myeloid or lymphoid malignancies (n=44781) were used for training and testing. **(a-b)** Baseline predictor included demographic characteristics (age, sex, smoking status, and genetic ethnic ancestry). CHIP (number of CHIP mutations and maximum VAF), mCA (number of alterations and maximum cell fraction), and CBC were added as predictors together with demographics. The values inside the parentheses indicate the AUC. Since A-mCA were associated with risk of both myeloid and lymphoid malignancies, these are combined with M-mCA in the analysis of myeloid malignancies and with L-mCA in the analysis of lymphoid malignancies. CLL, chronic lymphocytic leukemia; SLL, small lymphocytic lymphoma; CBC, complete blood count; VAF, variant allele fraction; AUC, area under the curve.

References

58. Morris, S.W., et al. Fusion of a kinase gene, ALK, to a nucleolar protein gene, NPM, in non-Hodgkin's lymphoma. *Science* 263, 1281-1284 (1994).
59. Wellmann, A., et al. Analysis of the t(2;5)(p23;q35) translocation by reverse transcription-polymerase chain reaction in CD30+ anaplastic large-cell lymphomas, in other non-Hodgkin's lymphomas of T-cell phenotype, and in Hodgkin's disease. *Blood* 86, 2321-2328 (1995).
60. Lamant, L., Dastugue, N., Pulford, K., Delsol, G. & Mariame, B. A new fusion gene TPM3-ALK in anaplastic large cell lymphoma created by a (1;2)(q25;p23) translocation. *Blood* 93, 3088-3095 (1999).
61. Siebert, R., et al. Complex variant translocation t(1;2) with TPM3-ALK fusion due to cryptic ALK gene rearrangement in anaplastic large-cell lymphoma. *Blood* 94, 3614-3617 (1999).
62. Chikatsu, N., et al. ALK+, CD30-, CD20- large B-cell lymphoma containing anaplastic lymphoma kinase (ALK) fused to clathrin heavy chain gene (CLTC). *Mod Pathol* 16, 828-832 (2003).
63. De Paepe, P., et al. ALK activation by the CLTC-ALK fusion is a recurrent event in large B-cell lymphoma. *Blood* 102, 2638-2641 (2003).
64. Gesk, S., et al. ALK-positive diffuse large B-cell lymphoma with ALK-Clathrin fusion belongs to the spectrum of pediatric lymphomas. *Leukemia* 19, 1839-1840 (2005).
65. Streubel, B., Vinatzer, U., Willheim, M., Raderer, M. & Chott, A. Novel t(5;9)(q33;q22) fuses ITK to SYK in unspecified peripheral T-cell lymphoma. *Leukemia* 20, 313-318 (2006).
66. Fujiwara, S.I., et al. High-resolution analysis of chromosome copy number alterations in angioimmunoblastic T-cell lymphoma and peripheral T-cell lymphoma, unspecified, with single nucleotide polymorphism-typing microarrays. *Leukemia* 22, 1891-1898 (2008).
67. Herens, C., et al. Cyclin D1-negative mantle cell lymphoma with cryptic t(12;14)(p13;q32) and cyclin D2 overexpression. *Blood* 111, 1745-1746 (2008).
68. Wlodarska, I., et al. Translocations targeting CCND2, CCND3, and MYCN do occur in t(11;14)-negative mantle cell lymphomas. *Blood* 111, 5683-5690 (2008).
69. Feldman, A.L., et al. Recurrent translocations involving the IRF4 oncogene locus in peripheral T-cell lymphomas. *Leukemia* 23, 574-580 (2009).
70. Morin, R.D., et al. Somatic mutations altering EZH2 (Tyr641) in follicular and diffuse large B-cell lymphomas of germinal-center origin. *Nat Genet* 42, 181-185 (2010).
71. Rui, L., et al. Cooperative epigenetic modulation by cancer amplicon genes. *Cancer Cell* 18, 590-605 (2010).
72. Feldman, A.L., et al. Discovery of recurrent t(6;7)(p25.3;q32.3) translocations in ALK-negative anaplastic large cell lymphomas by massively parallel genomic sequencing. *Blood* 117, 915-919 (2011).
73. Quesada, V., et al. Exome sequencing identifies recurrent mutations of the splicing factor SF3B1 gene in chronic lymphocytic leukemia. *Nat Genet* 44, 47-52 (2011).
74. Steidl, C. & Gascoyne, R.D. The molecular pathogenesis of primary mediastinal large B-cell lymphoma. *Blood* 118, 2659-2669 (2011).
75. Wang, L., et al. SF3B1 and other novel cancer genes in chronic lymphocytic leukemia. *N Engl J Med* 365, 2497-2506 (2011).

76. Greisman, H.A., et al. IgH partner breakpoint sequences provide evidence that AID initiates t(11;14) and t(8;14) chromosomal breaks in mantle cell and Burkitt lymphomas. *Blood* 120, 2864-2867 (2012).
77. Kridel, R., et al. Whole transcriptome sequencing reveals recurrent NOTCH1 mutations in mantle cell lymphoma. *Blood* 119, 1963-1971 (2012).
78. Love, C., et al. The genetic landscape of mutations in Burkitt lymphoma. *Nat Genet* 44, 1321-1325 (2012).
79. Vasmatazis, G., et al. Genome-wide analysis reveals recurrent structural abnormalities of TP63 and other p53-related genes in peripheral T-cell lymphomas. *Blood* 120, 2280-2289 (2012).
80. Woyach, J.A., Johnson, A.J. & Byrd, J.C. The B-cell receptor signaling pathway as a therapeutic target in CLL. *Blood* 120, 1175-1184 (2012).
81. Giacomini, C.P., et al. Breakpoint analysis of transcriptional and genomic profiles uncovers novel gene fusions spanning multiple human cancer types. *PLoS Genet* 9, e1003464 (2013).
82. Ying, C.Y., et al. MEF2B mutations lead to deregulated expression of the oncogene BCL6 in diffuse large B cell lymphoma. *Nat Immunol* 14, 1084-1092 (2013).
83. Bruno, A., et al. Mutational analysis of primary central nervous system lymphoma. *Oncotarget* 5, 5065-5075 (2014).
84. Gunawardana, J., et al. Recurrent somatic mutations of PTPN1 in primary mediastinal B cell lymphoma and Hodgkin lymphoma. *Nat Genet* 46, 329-335 (2014).
85. Hunter, Z.R., et al. The genomic landscape of Waldenstrom macroglobulinemia is characterized by highly recurring MYD88 and WHIM-like CXCR4 mutations, and small somatic deletions associated with B-cell lymphomagenesis. *Blood* 123, 1637-1646 (2014).
86. Muppidi, J.R., et al. Loss of signalling via Galpha13 in germinal centre B-cell-derived lymphoma. *Nature* 516, 254-258 (2014).
87. Parrilla Castellar, E.R., et al. ALK-negative anaplastic large cell lymphoma is a genetically heterogeneous disease with widely disparate clinical outcomes. *Blood* 124, 1473-1480 (2014).
88. Velusamy, T., et al. A novel recurrent NPM1-TYK2 gene fusion in cutaneous CD30-positive lymphoproliferative disorders. *Blood* 124, 3768-3771 (2014).
89. Braggio, E., et al. Genome-Wide Analysis Uncovers Novel Recurrent Alterations in Primary Central Nervous System Lymphomas. *Clin Cancer Res* 21, 3986-3994 (2015).
90. Crescenzo, R., et al. Convergent mutations and kinase fusions lead to oncogenic STAT3 activation in anaplastic large cell lymphoma. *Cancer Cell* 27, 516-532 (2015).
91. Kurtz, D.M., et al. Noninvasive monitoring of diffuse large B-cell lymphoma by immunoglobulin high-throughput sequencing. *Blood* 125, 3679-3687 (2015).
92. Vater, I., et al. The mutational pattern of primary lymphoma of the central nervous system determined by whole-exome sequencing. *Leukemia* 29, 677-685 (2015).
93. Yoda, A., et al. Mutations in G protein beta subunits promote transformation and kinase inhibitor resistance. *Nat Med* 21, 71-75 (2015).
94. Boddicker, R.L., et al. Integrated mate-pair and RNA sequencing identifies novel, targetable gene fusions in peripheral T-cell lymphoma. *Blood* 128, 1234-1245 (2016).
95. Chapuy, B., et al. Diffuse large B-cell lymphoma patient-derived xenograft models capture the molecular and biological heterogeneity of the disease. *Blood* 127, 2203-2213 (2016).

96. Chapuy, B., et al. Targetable genetic features of primary testicular and primary central nervous system lymphomas. *Blood* 127, 869-881 (2016).
97. Fukumura, K., et al. Genomic characterization of primary central nervous system lymphoma. *Acta Neuropathol* 131, 865-875 (2016).
98. Kridel, R., et al. Histological Transformation and Progression in Follicular Lymphoma: A Clonal Evolution Study. *PLoS Med* 13, e1002197 (2016).
99. Louissaint, A., Jr., et al. Pediatric-type nodal follicular lymphoma: a biologically distinct lymphoma with frequent MAPK pathway mutations. *Blood* 128, 1093-1100 (2016).
100. Morin, R.D., et al. Genetic Landscapes of Relapsed and Refractory Diffuse Large B-Cell Lymphomas. *Clin Cancer Res* 22, 2290-2300 (2016).
101. Rohr, J., et al. Recurrent activating mutations of CD28 in peripheral T-cell lymphomas. *Leukemia* 30, 1062-1070 (2016).
102. Yoo, H.Y., et al. Frequent CTLA4-CD28 gene fusion in diverse types of T-cell lymphoma. *Haematologica* 101, 757-763 (2016).
103. Grommes, C., et al. Ibrutinib Unmasks Critical Role of Bruton Tyrosine Kinase in Primary CNS Lymphoma. *Cancer Discov* 7, 1018-1029 (2017).
104. Lazarian, G., Guieze, R. & Wu, C.J. Clinical Implications of Novel Genomic Discoveries in Chronic Lymphocytic Leukemia. *J Clin Oncol* 35, 984-993 (2017).
105. Pedersen, M.B., et al. DUSP22 and TP63 rearrangements predict outcome of ALK-negative anaplastic large cell lymphoma: a Danish cohort study. *Blood* 130, 554-557 (2017).
106. Arthur, S.E., et al. Genome-wide discovery of somatic regulatory variants in diffuse large B-cell lymphoma. *Nat Commun* 9, 4001 (2018).
107. Hunter, Z.R., et al. Insights into the genomic landscape of MYD88 wild-type Waldenstrom macroglobulinemia. *Blood Adv* 2, 2937-2946 (2018).
108. Krumbholz, M., et al. Characterization and diagnostic application of genomic NPM-ALK fusion sequences in anaplastic large-cell lymphoma. *Oncotarget* 9, 26543-26555 (2018).
109. Vallois, D., et al. RNA fusions involving CD28 are rare in peripheral T-cell lymphomas and concentrate mainly in those derived from follicular helper T cells. *Haematologica* 103, e360-e363 (2018).
110. Chapuy, B., et al. Genomic analyses of PMBL reveal new drivers and mechanisms of sensitivity to PD-1 blockade. *Blood* 134, 2369-2382 (2019).
111. de Araujo, E.D., et al. Structural and functional consequences of the STAT5B(N642H) driver mutation. *Nat Commun* 10, 2517 (2019).
112. Gimenez, N., et al. Mutations in the RAS-BRAF-MAPK-ERK pathway define a specific subgroup of patients with adverse clinical features and provide new therapeutic options in chronic lymphocytic leukemia. *Haematologica* 104, 576-586 (2019).
113. Gruber, M., et al. Growth dynamics in naturally progressing chronic lymphocytic leukaemia. *Nature* 570, 474-479 (2019).
114. Guieze, R., et al. Mitochondrial Reprogramming Underlies Resistance to BCL-2 Inhibition in Lymphoid Malignancies. *Cancer Cell* 36, 369-384 e313 (2019).
115. Liang, W.S., et al. Comprehensive Genomic Profiling of Hodgkin Lymphoma Reveals Recurrently Mutated Genes and Increased Mutation Burden. *Oncologist* 24, 219-228 (2019).
116. Liu, Y. & Barta, S.K. Diffuse large B-cell lymphoma: 2019 update on diagnosis, risk stratification, and treatment. *Am J Hematol* 94, 604-616 (2019).

117. Martin-Garcia, D., et al. CCND2 and CCND3 hijack immunoglobulin light-chain enhancers in cyclin D1(-) mantle cell lymphoma. *Blood* 133, 940-951 (2019).
118. Onaindia, A., et al. DUSP22-rearranged anaplastic lymphomas are characterized by specific morphological features and a lack of cytotoxic and JAK/STAT surrogate markers. *Haematologica* 104, e158-e162 (2019).
119. Wright, G.W., et al. A Probabilistic Classification Tool for Genetic Subtypes of Diffuse Large B Cell Lymphoma with Therapeutic Implications. *Cancer Cell* 37, 551-568 e514 (2020).